



OPEN Analysis for type of 53BP1 nuclear expression by immunofluorescence as an indicator of genomic instability in oropharyngeal squamous epithelial lesions

Hideaki Nishi^{1,4}, Katsuya Matsuda^{2,4}, Mariko Terakado¹, Hisayoshi Kondo³, Yoshihiko Kumai¹ & Masahiro Nakashima²✉

A subset of oropharyngeal squamous cell carcinoma (OPSCC) is caused by the high-risk human papilloma virus (HPV), which expresses p16^{INK4a} immunoreactivity. Dual-color immunofluorescence (IF) analysis of TP53 binding protein-1 (53BP1) and a proliferative indicator, Ki-67, to elucidate genomic instability (GIN) in tumor tissues revealed that abnormal 53BP1 expression is closely associated with carcinogenesis in diverse organs. We have previously demonstrated that the number of 53BP1 nuclear foci (NF) in cervical cells increases with cancer progression. The distribution of 53BP1 NF was similar to that of punctate HPV signals, as determined by in situ hybridization, and the pattern of p16^{INK4a} overexpression. The present study aimed to confirm the type of 53BP1 expression using dual-color IF as an indicator of GIN in oropharyngeal squamous epithelial lesions, including HPV-dependent and -independent OPSCC. This study identified significant differences in the nuclear expression of 53BP1 between benign oropharyngeal epithelial lesions and OPSCC, and between HPV-dependent and HPV-independent OPSCC. We concluded that the incidence of abnormal 53BP1 expression in OPSCC is significantly associated with stage classification and overall survival. Therefore, double IF analysis of 53BP1 and Ki-67 expression may be a useful tool for estimating the malignant potential and prognosis of OPSCC.

Keywords Oropharyngeal squamous cell carcinoma, 53BP1, HPV, Genomic instability, p16^{INK4a}, p53

Oropharyngeal squamous cell carcinoma (OPSCC) is a type of head and neck cancer that affects the oropharynx, which includes the soft palate, uvula, palatine tonsils, posterior third (base) of the tongue, and posterior wall of the pharynx. OPSCC arises in the surface squamous mucosa, most commonly the tonsil (lateral wall)¹. Because of evidence that an increasing percentage of cases of OPSCC is caused by high-risk human papillomaviruses (HPV), the 4th edition of the WHO classification of tumors of the oropharynx classifies OPSCC into HPV-dependent and HPV-independent subtypes². p16^{INK4a} expression, analyzed using immunohistochemistry (IHC) studies, can be used as a surrogate marker for high-risk HPV as well as uterine cervical squamous lesions. In pathological practice, a lesion is classified as HPV-dependent OPSCC when p16^{INK4a} is found to be expressed in more than 70% of tumor cells on both nuclear and cytoplasmic staining³.

Clinicopathologically, there are several critical differences between the two subtypes. HPV-dependent OPSCC mainly affects the tonsillar crypts, is caused by high-risk HPV types 16 and 18, most commonly presents with basaloid features with no squamous differentiation, and is associated with an overall favorable prognosis despite early local lymph node metastasis^{3,4}. In HPV, early genes 1 (E1) and E2 activate viral replication, and oncoproteins encoded by genes E6 and E7 inactivate p53 and pRb tumor suppressor functions, respectively, promoting cellular proliferation and increasing the chance of malignancy⁵. In contrast, HPV-independent OPSCC most commonly arises on the surface mucosa of the soft palate (superior wall) and shows the typical

¹Department of Otolaryngology-Head and Neck Surgery, Nagasaki University Graduate School of Biomedical Sciences, 1-7-1 Sakamoto, Nagasaki 852-8501, Japan. ²Department of Tumor and Diagnostic Pathology, Atomic Bomb Disease Institute, Nagasaki University, 1-12-4 Sakamoto, Nagasaki 852-8523, Japan. ³Biostatistical Section, Atomic Bomb Disease Institute, Nagasaki University, 1-12-4 Sakamoto, Nagasaki 852-8523, Japan. ⁴These authors contributed equally: Hideaki Nishi and Katsuya Matsuda. ✉email: moemoe@nagasaki-u.ac.jp

	n	Median age \pm SD (range)	Male/Female	Smoker	Drinker
OPID	12	57.0 \pm 8.0 (41–69)	5/7	3 (25%)	4 (33.3%)
OPBT	4	58.5 \pm 3.4 (52–59)	2/2	2 (50%)	0
OPSCC	24	72.5 \pm 8.3 (54–88)	19/5	17 (70.8%)	16 (77.8%)

Table 1. Profiles of evaluated cases. SD: standard deviation; M: male; F: female; OPID: oropharyngeal inflammatory diseases; OPBT: oropharyngeal benign tumor; OPSCC: oropharyngeal squamous cell carcinoma.

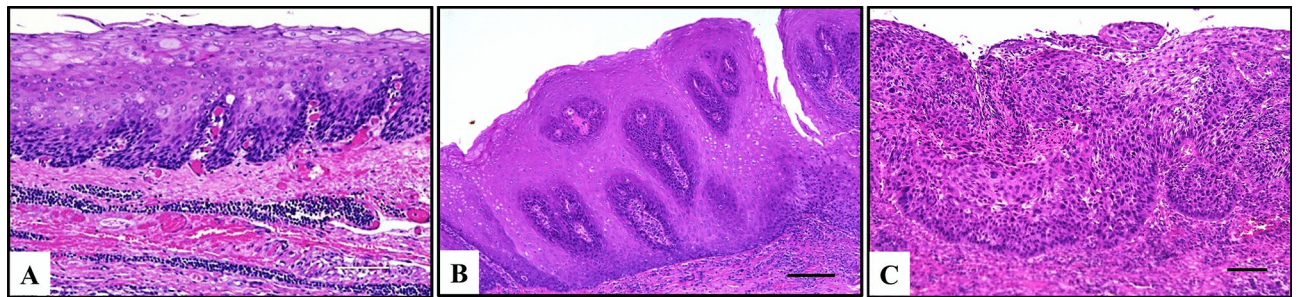


Fig. 1. Representative histological (hematoxylin and eosin-stained) images of oropharyngeal epithelial lesion. (A) Oropharyngeal inflammatory diseases. (B) Oropharyngeal benign tumor. (C) Oropharyngeal squamous cell carcinoma. The scale bars indicate 100 μ m.

morphology of conventional keratinizing squamous cell carcinoma (SCC) at any site¹. The incidence of HPV-independent OPSCC is associated with chronic injury owing to tobacco smoking, heavy alcohol use, and poor oral hygiene, inducing the abrogation of DNA repair mechanisms and p53 mutations⁶. Overall survival at 3 years for HPV-independent OPSCC is reported as 57%⁷.

TP53-binding protein 1 (53BP1), which belongs to the family of evolutionarily conserved DNA damage response (DDR) molecules, rapidly localizes at the sites of DNA double-strand breaks^{8,9} to activate the non-homologous end-joining repair machinery by working with other DDR molecules^{10–13}. Genomic instability (GIN), which is considered an important hallmark of malignant tumors, is occasionally evident in the precancerous stage of carcinogenesis^{14–17}. Given that the induction of endogenous DDR is a characteristic manifestation of GIN⁹, we propose that the measurement of 53BP1 expression can be a useful tool for estimating the level of GIN as well as the malignant potential of human tumors^{18–26}. We have previously demonstrated that the number of 53BP1 nuclear foci (NF) in uterine cervical cells increases with cancer progression¹⁸. Furthermore, the distribution of 53BP1 NF in uterine cervical cells was similar to that of punctate HPV signals, as determined by in situ hybridization and the pattern of p16^{INK4a} overexpression. These findings indicate that 53BP1 NF are associated with viral infection and replication stress. Dual-color immunofluorescence (IF) can be used to analyze 53BP1 expression, which in turn can be a useful indicator of GIN levels during cervical carcinogenesis¹⁸.

In a previous study, we had used IF to show that 53BP1 expression, including the number of NF that reflect endogenously occurring DDR, is altered during diverse tumorigenesis^{18–26}. In the current study, we analyzed 53BP1 expression using dual-color IF of 53BP1 and Ki-67 as a proliferative indicator in OPSCC tissues to estimate the level of GIN in oropharyngeal epithelial lesions, including HPV-dependent and -independent OPSCC. The present study identified significant differences in the nuclear expression of 53BP1 between benign oropharyngeal epithelial lesions and OPSCC, and HPV-dependent and HPV-independent OPSCC. We conclude that the incidence of abnormal 53BP1 expression in OPSCC is significantly associated with stage classification and overall survival (OS). This method can be an additive indicator to estimate OS of OPSCC with IHC for p16^{INK4a} expression.

Results

53BP1 expression in oropharyngeal squamous epithelial lesions

The clinical profiles of participants with oropharyngeal squamous epithelial lesions in this study are summarized in Table 1, and representative histological images of the oropharyngeal lesions are shown in Fig. 1. Representative images of 53BP1 expression obtained using dual-color IF are shown in Fig. 2. The results of IF analyses of 53BP1 expression in oropharyngeal squamous epithelial lesions are shown in Table 2, and representative images are shown in Fig. 3. The histological type of the oropharyngeal squamous epithelial lesion was significantly associated with both abnormal type 53BP1 expression and abnormal DDR type ($p < 0.0001$). In oropharyngeal inflammatory disease (OPID) cases, 88.9% of nuclei had stable type 53BP1 expression and only 3.2% of nuclei had abnormal type 53BP1 expression. Similarly, 86.0% of nuclei in oropharyngeal benign tumor (OPBT) cases showed stable expression, and 8.6% showed abnormal type 53BP1 expression. However, in OPSCC cases, 55.9% of nuclei had stable type and 31.4% of nuclei had abnormal type 53BP1 expression. The incidence of abnormal DDR type (53BP1 NF in Ki-67-positive cells) was also significantly higher in OPSCC (14.8%) than in OPID (1.5%) and OPBT (3.1%) ($p < 0.0001$).

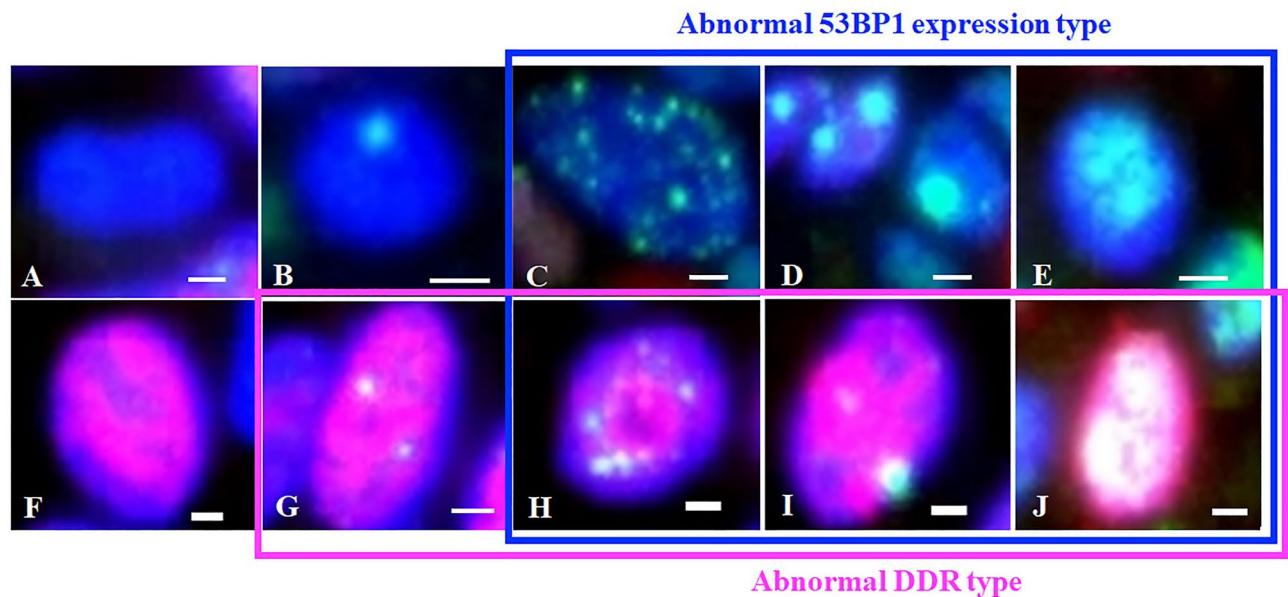


Fig. 2. Types of TP53-binding protein 1 expression (green) studied using dual-color immunofluorescence analysis with Ki-67 expression (red). (A & F) Stable DNA damage response (DDR) type—no or faint nuclear staining. (B & G) low DDR type—one or two discrete nuclear foci (NF). (C & H) high-DDR type—three or more discrete NF. (D & I)—large NF type, discrete NF larger than 1.0 μm . (E & J) diffuse type, intense heterogeneous nuclear staining. The incidence of high DDR, large foci, or diffuse types in the nuclei is considered as abnormal type 53BP1 expression^{18,21,24,26}. The incidence of colocalization of 53BP1 and Ki-67 expression (G–J) in nuclei is considered as abnormal DDR type. Because it is well known that DSBs induce cell cycle arrest, apoptosis, and/or senescence-like change, suggesting that 53BP1 NF should be normally induced in non-cycling cells^{30,31}. Scale bars indicate 2 μm .

53BP1 expression in OPSCC based on p16^{INK4a}/p53 expression

IHC studies revealed p16^{INK4a} expression and p53 expression in 14 (58.3%) and nine (37.5%) out of 24 OPSCC cases, respectively. Among these cases, two cases (8.3%) exhibited both p16^{INK4a} and p53 immunoreactivity, three cases (12.5%) exhibited neither p16^{INK4a} nor p53 immunoreactivity, 12 cases (50%) exhibited immunoreactivity only for p16^{INK4a} (p16^{INK4a}–single positive), and seven cases (29.2%) exhibited immunoreactivity only for p53 (p53–single positive). The number of OPSCC cases based on p16^{INK4a}/p53 expression results obtained using IHC is shown in Table 3.

The incidence of abnormal type 53BP1 expression was significantly higher in p53–single positive cases (38.4%) than in p16^{INK4a}–single positive cases (22.7%) ($p < 0.001$) (Fig. 4A). Similarly, the incidence of abnormal DDR type was significantly higher in p53–single positive cases (42.7%) than in p16^{INK4a}–single positive cases (29.5%) ($p < 0.001$) (Fig. 4B). Images of 53BP1 expression in each single case of combined p16^{INK4a}–positive/p53–negative and p16^{INK4a}–negative/p53–positive OPSCC are shown in Fig. 5.

53BP1 expression in OPSCC based on stage classification

Stage classification was performed for 19 OPSCC cases comprising 12 p16^{INK4a}–single positive cases and seven p53–single positive cases (Table 3) by according to the 8th edition the American Joint Committee on Cancer (AJCC) staging manual²⁷. Overall, there were five cases of Stage 0 or I, four cases of Stage II, six cases of Stage III, and four cases of Stage IV. The median incidence of abnormal type 53BP1 expression was 8.5% in Stage 0 or I, 30.6% in Stage II, 30.3% in Stage III, and 48.6% in Stage IV OPSCC cases (Fig. 6A). The median incidence of abnormal DDR type was 12.7% in Stage 0 or I, 31.3% in Stage II, 41.1% in Stage III, and 54.3% in Stage IV OPSCC cases (Fig. 6B). The Cochran–Armitage trend test revealed that the median incidences of both abnormal type 53BP1 expression and abnormal DDR type were significantly increased with stage progression (p for trend < 0.001).

Overall survival (OS) in OPSCC based on p16^{INK4a}/p53 expression and 53BP1 expression

The OS data was retrospectively obtained by assessing respective patient records, and compared between p16^{INK4a}–single positive and p53–single positive cases (Fig. 7A). Both 3-year and 5-year OS of p16^{INK4a}–single positive cases were 90.2%, while 3-year and 5-year OS of p53–single positive cases were 71.1% and 23.7%, respectively. This difference was statistically significant ($p < 0.001$).

Next, we focused on the incidence of abnormal type 53BP1 expression in oropharyngeal squamous epithelial lesions as an indicator to distinguish OPSCC or a marker for the classification of OPSCC, and examined the ROC curve. The area under the curve (AUC) value was 0.771 [95% confidence interval (CI), 0.494–1.000], suggesting reliable detection of malignancy. When an AUC of 54.2% was adopted as the cutoff value to diagnose OPSCC,

	n	Counted nuclei		Type of 53BP1 expression in all nuclei						Ki-67-positive nuclei		Type of 53BP1 expression in Ki-67-positive nuclei					
		Total	Case*	Stable	LDDR	HDDR	LF	Diffuse	Abnormal 53BP1			Stable	LDDR	HDDR	LF	Diffuse	Abnormal DDR
OPID	12	9198	735 ± 210 (456–1280)	8174 (88.9%)	726 (7.9%)	138 (1.5%)	110 (1.2%)	50 (0.5%)	298 (3.2%)	1703 (18.5%)		1569 (17.1%)	94 (1.0%)	18 (0.2%)	13 (0.1%)	9 (0.1%)	134 (1.4%)
OPBT	4	3479	915 ± 225 (561–1088)	2992 (86.0%)	188 (5.4%)	89 (2.6%)	151 (4.3%)	59 (1.7%)	299 (8.6%)	783 (22.5%)		674 (19.4%)	47 (1.4%)	28 (0.8%)	26 (0.7%)	8 (0.2)	109 (3.1%)
OPSCC	24	21,975	889 ± 282 (462–1457)	12,284 (55.9%)	2787 (12.7%)	1643 (7.5%)	3246 (14.8%)	2015 (9.2%)	6904 (31.4%)	8125 (37.0%)		4883 (22.2%)	909 (4.1%)	699 (3.2%)	925 (4.2%)	709 (3.2%)	3242 (14.7%)

Table 2. Types of TP53-binding protein 1 (53BP1) expression observed in oropharyngeal squamous epithelial lesions by dual-color IF analysis. IF: immunofluorescence; OPID: oropharyngeal inflammatory diseases; OPBT: oropharyngeal benign tumor; OPSCC: oropharyngeal squamous cell carcinoma; LDDR: low DNA damage response; HDDR: high DNA damage response; LF: large foci. *Counted nuclei per case: median ± standard deviation (range).

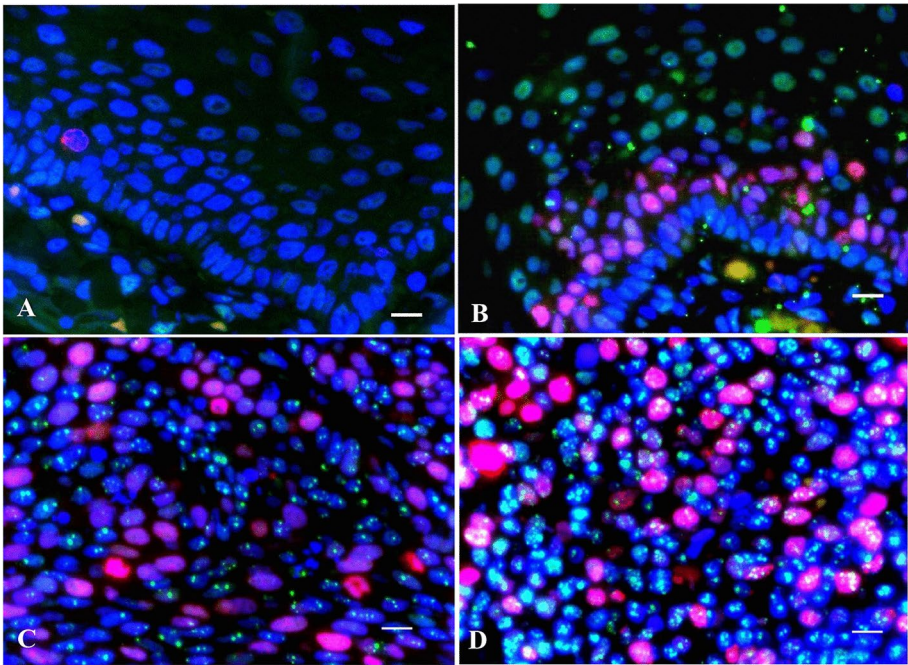


Fig. 3. Dual-labeled immunofluorescence of TP53-binding protein 1 (green) and Ki-67 (red) expression in oropharyngeal epithelial lesions. (A) Oropharyngeal inflammatory disease. (B) Oropharyngeal benign tumor. (C) P16^{INK4a}-positive oropharyngeal squamous cell carcinoma (OPSCC). (D) P16^{INK4a}-negative OPSCC. The scale bars indicate 10 μm.

	P53 positive	P53 negative	
P16 positive	2 (8.3)	12 (50%)	14 (58.3%)
P16 negative	7 (29.2%)	3 (12.5%)	10 (41.7%)
	9 (37.5%)	15 (62.5%)	24 (100%)

Table 3. Case number of oropharyngeal squamous cell carcinoma based on p16/p53 expressions by immunohistochemistry.

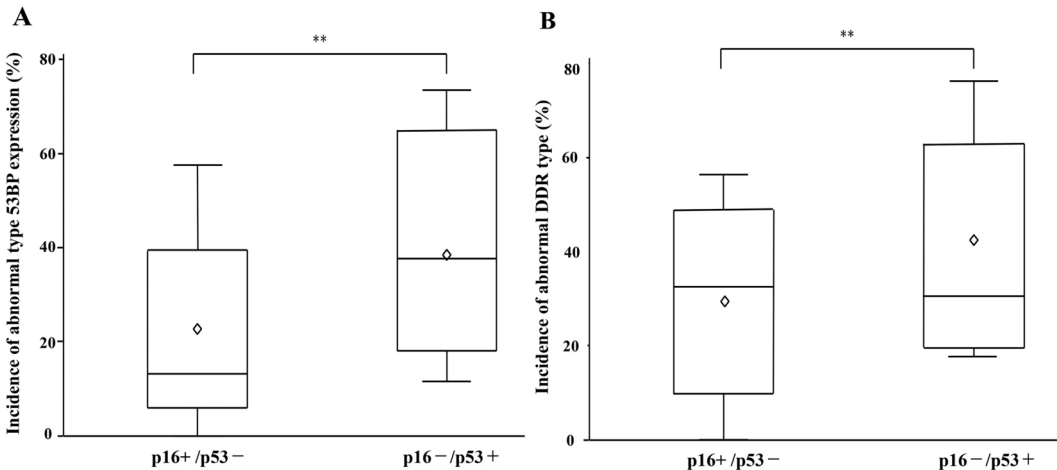


Fig. 4. Comparison of median incidences of abnormal TP53-binding protein 1 (53BP1) expression in p16^{INK4a}-dependent and -independent oropharyngeal squamous cell carcinoma (OPSCC). OPSCC ***p* < 0.001 by chi-square test. White square indicates the mean value.

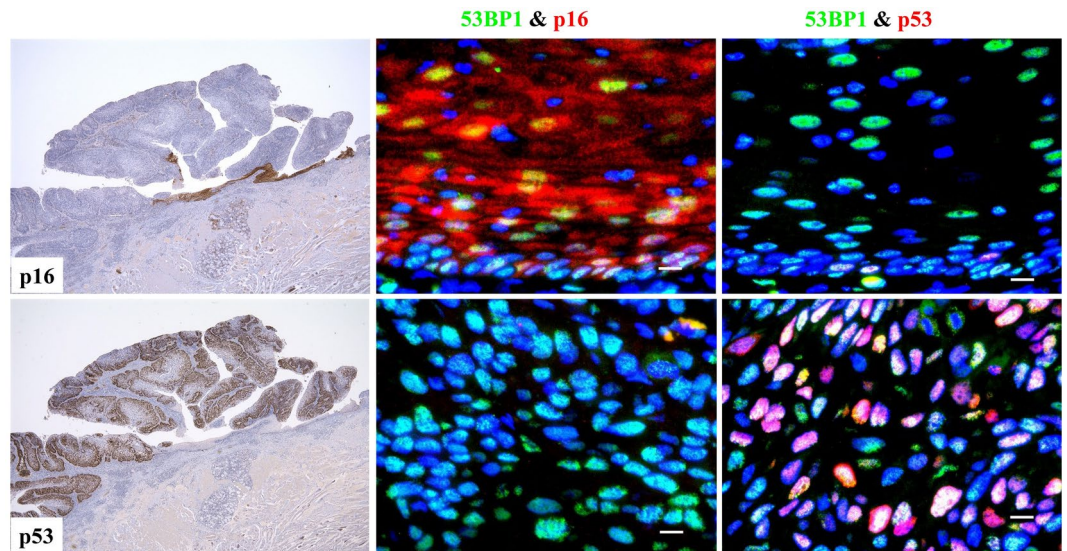


Fig. 5. Comparison of type of TP53-binding protein-1 (53BP1) (green) expression in a case of combined p16^{INK4a}-positive/ p53-negative (upper panels) and p16^{INK4a}-negative/ p53-positive (lower panels) oropharyngeal squamous cell carcinoma. Abnormal type 53BP1 expression is significantly increased in lower panels compared with that in upper panels. The scale bars indicate 10 μ m.

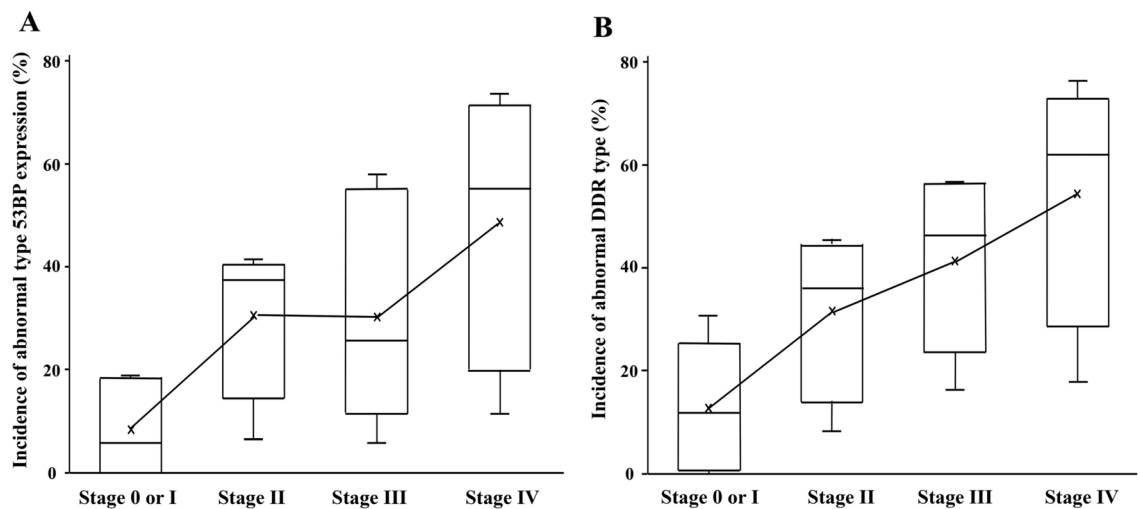


Fig. 6. Comparison of median incidences of abnormal TP53-binding protein 1 (53BP1) expression in oropharyngeal squamous cell carcinoma based on the Stage classification (AJCC 8th edition). Cochran-Armitage trend test revealed that median incidences of both abnormal type 53BP1 expression (A) and abnormal DNA damage response (DDR) type (B) are significantly increased with stage progression. p -values for trend < 0.001 by Cochran-Armitage test.

the sensitivity and specificity were 60% and 99.3%, respectively. Using the cutoff value mentioned above, we divided the 24 cases of OPSCC into two groups, namely, low and high abnormal type 53BP1 expression, and calculated OS. The results showed that 3-year and 5-year OS of low abnormal type 53BP1 expression group were 93.8% and 80.0%, respectively, whereas those of high abnormal type 53BP1 expression group were 42.8% and 42.7%, respectively (Fig. 7B). The differences for both 3-year and 5-year OS were statistically significant ($p < 0.02$).

Furthermore, the cutoff value was similarly estimated for the incidence of abnormal DDR. The AUC value was 0.729 (95% CI, 0.447–1.000), suggesting reliable detection of OPSCC. When 56.0% was adopted as the cutoff value to diagnose malignancy, the sensitivity and specificity were 60% and 99.3%, respectively. Using the cutoff value calculated above, we divided the 24 cases of OPSCC into two groups, namely, low and high expression, and calculated OS. The 3-year and 5-year OS of low expression group were 84.3% and 72.1%, respectively, whereas

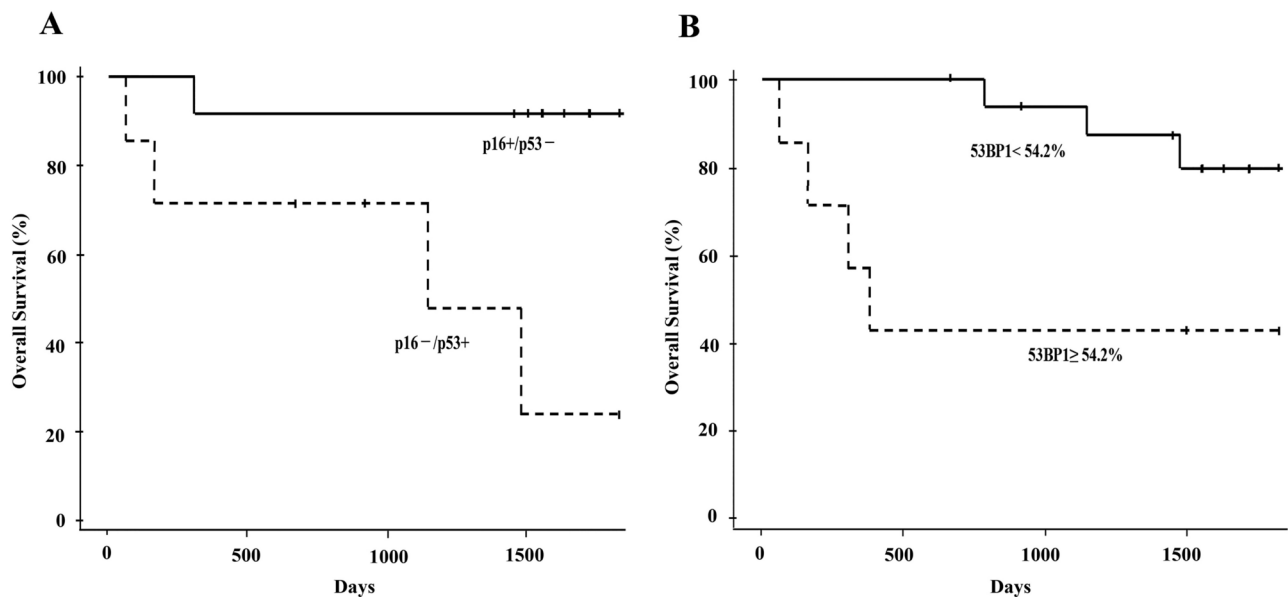


Fig. 7. Comparison of overall survival rate in p16^{INK4a}-dependent and -independent oropharyngeal squamous cell carcinoma (**A**) and based on median incidences of abnormal type TP53-binding protein 1 (53BP1) expression with the cutoff value of 54.2% (**B**). P16^{INK4a}-independent (p53-positive) cases show a worse prognosis compared with p16^{INK4a}-dependent (p53-negative) cases. Cases exhibiting a high (> 54.2%) abnormal type 53BP1 expression show a worse prognosis compared with those exhibiting a low (< 54.2%) abnormal type 53BP1 expression. *p*-value < 0.01 by log-rank test.

Factor	OR	95% CI
Type of 53BP1 expression by IF		
Abnormal 53BP1 expression type > 54%	19.500	(1.299, 292.750)
Abnormal DDR type > 56%	9.000	(0.873, 92.759)
P16 ^{INK4a} positive by IHC	0.068	(0.005, 0.861)
P53 positive by IHC	14.667	(1.161, 185.234)

Table 4. OR and 95% CI of respective factor for oropharyngeal squamous cell carcinoma-specific death estimated by logistic regression model. OR: Odds ratio; CI: confidence interval; IF: immunofluorescence; DDR: DNA damage response; IHC: immunohistochemistry.

both 3-year and 5-year OS of high expression group were 49.3%. This difference was not statistically significant (*p* = 0.234).

Odds ratio (OR) of each factor for OPSCC-specific death estimated by logistic regression model

OR and 95% CI of each factor, such as types of 53BP1 expression and p16^{INK4a}/ p53 expression, for OPSCC-specific death were estimated using a logistic regression model and the results are summarized in Table 4. Statistical significance was detected between abnormal type 53BP1 expression, p16^{INK4a} expression, and p53 expression. OR for the incidence of abnormal type 53BP1 expression (cutoff value, 54%) was largest among these factors.

Discussion

This study provided results establishing the significance of 53BP1 expression as a histological indicator for OPSCC in comparisons of OPID and OPBT, and p16^{INK4a}/ p53 expression in OPSCC. Our results clearly demonstrated that both abnormal type 53BP1 expression and abnormal DDR type were significantly higher in OPSCC than in OPID or OPBT. A higher incidence of nuclei showing abnormal type 53BP1 expression (cutoff value 54.2%) could specifically (99.3%) distinguish OPSCC from other benign lesions, indicating the significance of 53BP1 expression to estimate the malignant potential of oropharyngeal lesions. Our previous studies have demonstrated a correlation between the nuclear expression of 53BP1 and the malignant potential of human tumors, including SCC, such as skin²⁰, uterine cervical¹⁸, esophageal²³, and oral cancers²⁴. Thus, IF analysis for type of 53BP1 expression can be a reliable histological indicator to estimate the malignant potential of oropharyngeal squamous epithelial lesions, as well as squamous lesions at other sites.

Furthermore, the present study revealed an increased incidence of both abnormal type 53BP1 expression and abnormal DDR type in p53–single positive cases than in p16^{INK4a}–single positive cases, suggesting a higher level of GIN status in the HPV-independent p53-positive subtype than in the HPV-dependent p16^{INK4a}–positive subtype. In a previous study, we had proposed that double IF analysis of 53BP1 and Ki-67 expression could be a useful tool for estimating chromosomal instability, by detecting copy number alterations (CNA), and thereby the malignant potential of urothelial tumors, using multicolored fluorescence in situ hybridization (FISH)²¹. In urothelial carcinoma (UC), a higher incidence of nuclei with abnormal 53BP1 expression plus Ki-67 immunoreactivity (abnormal DDR type) indicated high-grade UC, which exhibited CNA, and p53 overexpression, and was p16^{INK4a}–negative. In contrast, low-grade UC exhibited p16^{INK4a} immunoreactivity. These characteristics allowed distinguishing high-grade UC from low-grade UC with 80% sensitivity and 100% specificity²¹. Taken together, the loss of normal p16^{INK4a} as a downregulator of replication stress and disruption of p53 activity as a key effector in the DDR machinery were associated with malignant transformation and progression, respectively, with GIN in HPV-independent OPSCC as well as high-grade UC.

Additionally, our cohort included three cases of HPV-independent p53-negative subtype as shown in Table 3. Profiles of these three cases were summarized in Supplementary Table S1. This result demonstrated that all these cases were heavy smoker and drinker, advanced stage, and exhibited high levels of both abnormal type of 53BP1 expression and abnormal DDR type. One case among them deceased by disease-specific cause. Thus, HPV-independent cases seem to be associated with both smoking history and abnormal 53BP1 expression, which should be a risk factor for poor prognosis regardless of status of TP53.

This study also demonstrated a stepwise increase in the incidence of nuclei exhibiting abnormal type 53BP1 expression and abnormal DDR types with advancing stages of OPSCC. When 54.2% was adopted as a cutoff value in OPSCC, cases with a higher incidence of nuclei showing abnormal type 53BP1 expression exhibited significantly worse OS. Additionally, our statistical analysis with a logistic regression model demonstrated that abnormal type 53BP1 expression in OPSCC by dual-color IF was a strong risk factor for OPSCC-specific death (OR, 19.500). Similarly, p53-positivity by IHC was revealed to be a strong risk factor for OPSCC-specific death (OR, 14.667). Conversely, p16^{INK4a} positivity in OPSCC by IHC (HPV-dependent subtype) was significantly associated with a better prognosis (OR, 0.068).

The major limitation of this study is that it was retrospectively conducted in a single institute with a small sample size. A prospective study with a larger cohort is required to recommend the procedures applied in this study for routine diagnostic use. In spite of this limitation, this study provides evidence of endogenously occurring DNA DSBs or altered DDR in oropharyngeal squamous epithelial lesions, similar to other malignancies at any site^{18–26}. The type of 53BP1 expression, such as abnormal type 53BP1 expression and abnormal DDR type, is associated with not only the malignant potential of oropharyngeal squamous epithelial lesions, but also the subtype and prognosis of OPSCC, thereby influencing clinical management. It is currently evident that HPV-dependent OPSCC is associated with a significantly better outcome regardless of the treatment strategy, and treatment de-escalation strategies are highly desired and sought-after^{28,29}. Therefore, a new biological indicator is required to estimate better prognosis for OPSCC. Thus, we propose that double IF analysis of 53BP1 and Ki-67 expression is a useful tool for estimating the malignant potential of oropharyngeal squamous epithelial lesions and prognosis of patients with OPSCC. The use of this tool will enable more accurate prognosis and early selection of appropriate treatment strategies for patients with OPSCC.

Methods

Participants

A total of 40 cases of oropharyngeal lesions, including chronic tonsillitis (n = 12), squamous papilloma (n = 4) and squamous cell carcinoma (SCC) (n = 24), were included in this study. All samples were formalin-fixed and paraffin-embedded tissues that were biopsied or obtained via surgically resection at the Nagasaki University Hospital between 2016 and 2019. Patients with the past history of pre-treatments, such as chemotherapy and radiotherapy, were excluded in this study. The pathological diagnoses of all samples were re-confirmed by a certified pathologist (M.N.) according to the 4th WHO Classification of Head and Neck Tumours².

IF analysis for 53BP1 expression

53BP1 nuclear expression was examined using dual-color IF analysis with Ki-67 expression, as the representative marker for cycling cells, to assess the extent and integrity of DDR according to our previous reports^{18–26}. Briefly, for dual-color IF, after blocking for non-specific reaction, the deparaffinized tissue sections were incubated with anti-53BP1 rabbit polyclonal antibody (1:1000; A200-272A; Bethyl Laboratories, Montgomery, TX, USA) and anti-Ki-67 mouse antibody (1:50; MIB-1; DakoCytomation, Glostrup, Denmark) for 1 h at 20 °C^{18–26}. The samples were then incubated with Alexa Fluor® 488-conjugated goat anti-rabbit and Alexa Fluor® 546-conjugated goat anti-mouse antibodies (1:2000; Invitrogen, Carlsbad, CA, USA), and mounted using VECTASHIELD® HardSet™ Mounting Medium with DAPI (Vector Laboratories, Burlingame, CA, USA)^{18–26}. The minimum 25 slices of stained sections per field were photographed at 1000-fold magnification using the Z-stack function on fluorescence microscope equipped with image analysis software (Bioevo BZ-X710; KEYENCE, Osaka, Japan), which enabled the delineation of all 53BP1 NF in the nucleus^{18–26}. The 53BP1 signals were measured using the Bioevo BZ-X710 microscope. The percentage of nuclei with each type of 53BP1 immunoreactivity was calculated in at least ten consecutive fields along the basement membrane of each lesion.

Classification of type of 53BP1 expression by IF

According to our previous study^{18,21,24,26}, 53BP1 immunoreactivity can be classified into five types based on the number and size of NF—(i) stable type: no or faint nuclear staining, (ii) low DDR type: one or two discrete NF, (iii) high DDR type: three or more discrete NF, (iv) large NF type: discrete NF larger than 1.0 µm, and (v)

diffuse type: intense heterogeneous nuclear staining. In the present study, types (iii), and both (iv) and (v) were considered as abnormal type 53BP1 expression. In addition, nuclei showing co-localization of 53BP1 NF and Ki-67, as a reliable indicator for cycling cells, in the double staining study were considered abnormal DDR type (Fig. 2). Genomic integrity can be threatened by both spontaneous and induced DNA damage, to which normal cells respond by activating a fine-tuned DDR, which regulates several processes^{30,31}. As DDR is normally associated with cell cycle arrest, apoptosis, and senescence^{30,31}, the co-expression of 53BP1 NF and Ki-67 can be considered an indicator of an impaired DDR pathway. Indeed, our previous results revealed frequent co-localization of 53BP1 NF and Ki-67 expression in cancer cell nuclei but rare in surrounding normal cells of several organs, suggesting perturbed DDR during carcinogenesis^{18,21–26}.

IHC for p53 and p16^{INK4a} expressions

Deparaffinized 4-μm sections were pre-treated by heating in a microwave in a phosphate buffer (pH 9.0) for 20 min, then incubated with mouse anti-p53 monoclonal antibody (1:200; Leica Biosystems, Nussloch, Germany) or mouse anti-p16^{INK4a} monoclonal antibody (1:2; Roche Diagnostics, Basel, Switzerland) for 15 min at 37 °C. After incubation for 8 min with the primary reagent of the Bond Polymer System (Leica Biosystems), the samples were incubated with the polymer reagent (peroxidase-labeled polymer-conjugated anti-mouse and anti-rabbit polyclonal antibodies) for 8 min. All samples were then incubated with 3,3'-diaminobenzidine hydrogen peroxide for 10 min and counterstained with hematoxylin. Immunoreactivity for p16/p53 expression was judged as positive when lesion showed a clear block-positivity by lower magnification.

Statistical analyses

Associations between the histological type of the oropharyngeal lesion, type of 53BP1 expression, and levels of p16^{INK4a} and p53 immunoreactivity were assessed using Jonckheere–Terpstra, Cochran–Armitage, and chi-square tests, respectively. A logistic regression model and receiver operating characteristic (ROC) curve were used to evaluate the significance of abnormal 53BP1 expression by dual-color IF, and p16^{INK4a} and p53 expression by IHC as diagnostic tests for estimating OPSCC-specific death. The closest distance from the top-left corner (point (0,1)) was used to identify the optimal cutoff value on the ROC curve. The overall survival rate was calculated using the Kaplan–Meier method, and differences in survival were analyzed using the log-rank test. The PHREG procedure in the SAS 8.2 software (SAS Institute, Cary, NC, USA) was used for this calculation. All tests were two-tailed, and a *p*-value < 0.05 was considered statistically significant.

Data availability

The datasets used and/or analysed during the current study available from the corresponding author on reasonable request.

Received: 26 May 2024; Accepted: 28 October 2024

Published online: 11 November 2024

References

1. Nibu, K.-I. et al. (eds) *Report of Head and Neck Cancer Registry of Japan Clinical Statistics of Registered Patients* (Japan Society for Head and Neck Cancer, 2023).
2. El-Naggar, A. K., Chan, J. K. C., Grandis, K. R., Takata, T. & Slootweg, P. *WHO Classification of Head and Neck Tumours* 4th edn. (IARC Press, 2017).
3. Holzinger, D. et al. Identification of oropharyngeal squamous cell carcinomas with active HPV16 involvement by immunohistochemical analysis of the retinoblastoma protein pathway. *Int. J. Cancer* **133**, 1389–1399 (2013).
4. Westra, W. H. The morphologic profile of HPV-related head and neck squamous carcinoma: implications for diagnosis, prognosis, and clinical management. *Head Neck Pathol.* **6**(Suppl 1), S48–S54 (2012).
5. Allison, D. B. & Maleki, Z. HPV-related head and neck squamous cell carcinoma: An update and review. *J. Am. Soc. Cytopathol.* **5**, 203–215 (2016).
6. Tanaka, T. & Ishigamori, R. Understanding carcinogenesis for fighting oral cancer. *J. Oncol.* **2011**, 603740 (2011).
7. Ang, K. K. et al. Human papillomavirus and survival of patients with oropharyngeal cancer. *N. Engl. J. Med.* **363**, 24–35 (2010).
8. Schultz, L. B., Chehab, N. H., Malikzay, A. & Halazonetis, T. D. P53 binding protein 1 (53BP1) is an early participant in the cellular response to DNA double-strand breaks. *J. Cell Biol.* **151**, 1381–1390 (2000).
9. Suzuki, K., Yokoyama, S., Waseda, S., Kodama, S. & Watanabe, M. Delayed reactivation of p53 in the progeny of cells surviving ionizing radiation. *Cancer Res.* **63**, 936–941 (2003).
10. Cao, L. et al. A selective requirement for 53BP1 in the biological response to genomic instability induced by BRCA1 deficiency. *Mol. Cell* **35**, 534–541 (2009).
11. Bunting, S. F. et al. 53BP1 inhibits homologous recombination in BRCA1-deficient cells by blocking resection of DNA breaks. *Cell* **141**, 243–254 (2010).
12. Bouwman, P. et al. 53BP1 loss rescues BRCA1 deficiency and is associated with triple-negative and BRCA-mutated breast cancers. *Nat. Struct. Mol. Biol.* **17**, 688–695 (2010).
13. Bunting, S. F. et al. BRCA1 functions independently of homologous recombination in DNA interstrand crosslink repair. *Mol. Cell* **46**, 125–135 (2012).
14. Lengauer, C., Kinzler, K. W. & Vogelstein, B. Genetic instabilities in human cancers. *Nature* **396**, 643–649. <https://doi.org/10.1038/25292> (1998).
15. Zhu, C. et al. Unrepaired DNA breaks in p53-deficient cells lead to oncogenic gene amplification subsequent to translocations. *Cell* **109**, 811–821. [https://doi.org/10.1016/S0092-8674\(02\)00770-5](https://doi.org/10.1016/S0092-8674(02)00770-5) (2002).
16. Coleman, W. B. & Tsongalis, G. J. The role of genomic instability in human carcinogenesis. *Anticancer Res.* **19**, 4645–4664 (1999).
17. Negrini, S., Gorgoulis, V. G. & Halazonetis, T. D. Genomic instability—an evolving hallmark of cancer. *Nat. Rev. Mol. Cell Biol.* **11**, 220–228. <https://doi.org/10.1038/nrm2858> (2010).
18. Matsuda, K. et al. Significance of p53-binding protein 1 nuclear foci in uterine cervical lesions: Endogenous DNA double strand breaks and genomic instability during carcinogenesis. *Histopathology* **59**, 441–451 (2011).
19. Nakashima, M. et al. Foci formation of P53-binding protein 1 in thyroid tumors: activation of genomic instability during thyroid carcinogenesis. *Int. J. Cancer* **122**, 1082–1088 (2008).

20. Naruke, Y. et al. Alteration of p53-binding protein 1 expression during skin carcinogenesis: association with genomic instability. *Cancer Sci.* **99**, 946–951 (2008).
21. Matsuda, K. et al. Expression pattern of p53-binding protein 1 as a new molecular indicator of genomic instability in bladder urothelial carcinoma. *Sci. Rep.* **8**, 15477 (2018).
22. Otsubo, R. et al. A novel diagnostic method for thyroid follicular tumors based on immunofluorescence analysis of p53-binding protein 1 expression: detection of genomic instability. *Thyroid* **29**, 657–665 (2019).
23. Ueki, N. et al. Significant association between 53 BP1 expression and grade of intraepithelial neoplasia of esophagus: alteration during esophageal carcinogenesis. *Pathol. Res. Pract.* **215**, 152601 (2019).
24. Imaizumi, T. et al. Detection of endogenous DNA double-strand breaks in oral squamous epithelial lesions by P53-binding protein 1. *Anticancer Res.* **41**, 4771–4779 (2021).
25. Luong, T. M. H. et al. Significance of abnormal 53BP1 expression as a novel molecular pathologic parameter of follicular-shaped B-cell lymphoid lesions in human digestive tract. *Sci. Rep.* **11**, 3074 (2021).
26. Ueda, M. et al. Molecular pathological characteristics of thyroid follicular-patterned tumors showing nodule-in-nodule appearance with poorly differentiated component. *Cancers (Basel)*. **14**(15), 3577. <https://doi.org/10.3390/cancers14153577> (2022).
27. Amin, M. B. et al. (eds) *AJCC Cancer Staging Manual* 8th edn. (Springer International Publishing, 2017).
28. Gillison, M. L. et al. Evidence for a causal association between human papillomavirus and a subset of head and neck cancers. *J. Natl. Cancer Inst.* **92**, 709–720–203074 (2000).
29. Golusinski, P. et al. De-escalation studies in HPV-positive oropharyngeal cancer: How should we proceed?. *Oral Oncol.* **123**, 105620 (2021).
30. Fortini, P., Ferretti, C. & Dogliotti, E. The response to DNA damage during differentiation: pathways and consequences. *Mutat. Res.* **743–744**, 160–168 (2013).
31. Trovesi, C., Manfrini, N., Falcattoni, M. & Longhese, M. P. Regulation of the DNA damage response by cyclin-dependent kinases. *J. Mol. Biol.* **425**, 4756–4766 (2013).

Author contributions

H.N., Y.K., and M.N. wrote the main manuscript text and H.N. and K.M. prepared figures. H.N., K.H., and M.T. carried out experiments, interpreted results, and summarised all of data. All authors reviewed and approved the manuscript.

Funding

This work was funded by the Atomic Bomb Disease Institute Nagasaki University, and the Program of the Network-Type Joint Usage/Research Center for Radiation Disaster Medical Science.

Declarations

Competing interests

The authors declare no competing interests.

Ethics committee approval and informed consent

This study was performed retrospectively in accordance with the tenets of the Declaration of Helsinki. The Ethics Committee of Nagasaki university hospital approved the study (approval date: November 20, 2018; #18111921) and waived the need for informed consent. All methods were carried out in accordance with relevant guidelines and regulations. Patient profiles were anonymized by coding and collectively summarized with the obtained data as the final dataset. Patients were able to opt out of the study by following the instructions provided on the institute website.

Additional information

Supplementary Information The online version contains supplementary material available at <https://doi.org/10.1038/s41598-024-77945-y>.

Correspondence and requests for materials should be addressed to M.N.

Reprints and permissions information is available at www.nature.com/reprints.

Publisher's note Springer Nature remains neutral with regard to jurisdictional claims in published maps and institutional affiliations.

Open Access This article is licensed under a Creative Commons Attribution-NonCommercial-NoDerivatives 4.0 International License, which permits any non-commercial use, sharing, distribution and reproduction in any medium or format, as long as you give appropriate credit to the original author(s) and the source, provide a link to the Creative Commons licence, and indicate if you modified the licensed material. You do not have permission under this licence to share adapted material derived from this article or parts of it. The images or other third party material in this article are included in the article's Creative Commons licence, unless indicated otherwise in a credit line to the material. If material is not included in the article's Creative Commons licence and your intended use is not permitted by statutory regulation or exceeds the permitted use, you will need to obtain permission directly from the copyright holder. To view a copy of this licence, visit <http://creativecommons.org/licenses/by-nc-nd/4.0/>.

© The Author(s) 2024